Scaling behavior and parasitic series resistance in disordered organic field-effect transistors

E. J. Meijer[a)]
Philips Research Laboratories, 5656 AA Eindhoven, The Netherlands and Delft University of Technology, Faculty of Applied Sciences, Department of NanoScience, Lorentzweg 1 2628 CJ Delft, The Netherlands

G. H. Gelinck, E. van Veenendaal, B.-H. Huisman, and D. M. de Leeuw
Philips Research Laboratories, 5656 AA Eindhoven, The Netherlands

T. M. Klapwijk
Delft University of Technology, Faculty of Applied Sciences, Department of NanoScience, Lorentzweg 1 2628 CJ Delft, The Netherlands

(Received 13 February 2003; accepted 9 April 2003)

The scaling behavior of the transfer characteristics of solution-processed disordered organic thin-film transistors with channel length is investigated. This is done for a variety of organic semiconductors in combination with gold injecting electrodes. From the channel-length dependence of the transistor resistance in the conducting ON-state, we determine the field-effect mobility and the parasitic series resistance. The extracted parasitic resistance, typically in the MΩ range, depends on the applied gate voltage, and we find experimentally that the parasitic resistance decreases with increasing field-effect mobility. © *2003 American Institute of Physics.*
[DOI: 10.1063/1.1581389]

The interest in organic thin-film transistors (TFTs) has grown rapidly due to envisaged applications, such as integrated circuits[1] and active-matrix displays.[2] The switching speed of organic integrated circuits can be estimated from the performance of the individual transistors and is roughly proportional to $\sim \mu_{\mathrm{FE}}/L^2$,[3] where L is the channel length of the transistor, and μ_{FE} is the field-effect mobility. To reach higher switching speeds, the search for higher mobility materials is therefore important, but it is also of great interest to downsize the transistor geometries. In this work, the scaling behavior of the transfer characteristics with transistor channel length is investigated for a variety of solution-processable organic TFTs.

In the experiments, we use heavily doped Si wafers as the gate electrode, with a 200-nm-thick layer of thermally oxidized SiO_2 as the gate-insulating layer. Using conventional lithography, gold source and drain contacts 100 nm thick are defined, with channel widths ranging from 1 mm to 1 cm and channel lengths between 0.75 and 40 μm. The structures typically have an underetch of 0.5 μm, which we neglect in the following analysis. A 10-nm layer of titanium acts as an adhesion layer for the gold on the SiO_2. The SiO_2 layer is treated with the primer hexamethyldisilazane to make the surface hydrophobic. No special care is taken to clean the gold surface prior to deposition of the semiconductor. Poly(2,5-thienylene vinylene) (PTV) films as semiconductor layer are deposited using a precursor-route process.[3] We systematically varied the processing conditions for the conversion from precursor to PTV, and we determined the average degree of conversion using the method described by Fuchigami *et al.*[4] This enabled us to systematically study PTV transistors at various degrees of conversion ranging from 60% to 100%, and consequently over a range of field-effect mobilities, between 10^{-4} and 10^{-3} cm^2/V s. Poly(3-hexyl thiophene) (P3HT) is spin-coated from a 1 wt % chloroform solution. Films of poly([2-methoxy-5-(3′,7′-dimethyloctyloxy)]-*p*-phenylene vinylene) (OC_1C_{10}-PPV) and poly([2,5-di-(3′,7′-dimethyloctyloxy)]-*p*-phenylene vinylene) ($OC_{10}C_{10}$-PPV), are spun from a 0.5 wt % toluene solution. Pentacene thin films are deposited using a precursor-route process.[3] The measurements are performed on freshly prepared samples in order to minimize external doping and degradation effects.[5] The PTV, OC_1C_{10}-PPV, $OC_{10}C_{10}$-PPV, and pentacene samples are measured in air, whereas the P3HT samples are measured in vacuum and dark after a thermal dedope procedure.[6] The electrical characteristics are recorded using an HP4155B semiconductor parameter analyzer.

Typical source–drain current I_{ds} versus gate voltage V_g characteristics for solution-processed PTV and P3HT are shown in Fig. 1 for different channel lengths, where W is kept constant. The position of the switch-on voltage V_{so},[7] which determines the onset of the field effect and is defined as the flatband condition of the transistor, does not vary much between the transistors with different channel length. At low source–drain voltage, $V_{\mathrm{ds}} = -2$ V, where the in-plane drift field is much smaller than the applied gate field (gradual channel approximation),[3] the field-effect mobility is evaluated using

$$\mu_{\mathrm{FE}}(V_g) = \frac{L}{WC_iV_{\mathrm{ds}}}\frac{\partial I_{\mathrm{ds}}}{\partial V_g}, \tag{1}$$

where W is the channel width and C_i the capacitance of the insulating layer per unit area.

a)Electronic mail: eduard.meijer@philips.com

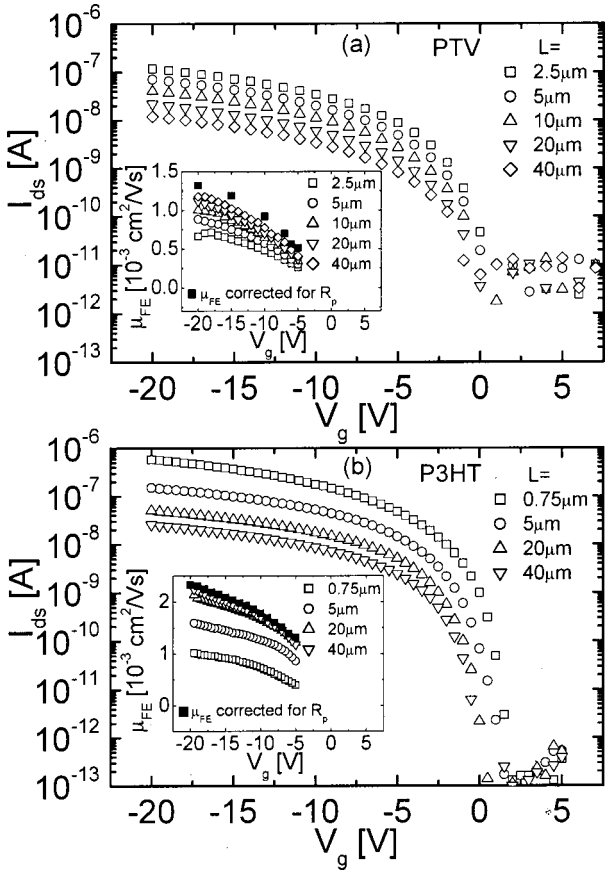

FIG. 1. I_{ds} vs V_g at $V_{ds}=-2$ V, for different channel lengths for (a) PTV, converted at 80 °C under 150 mbar of HCl partial pressure (see Ref. 3). The characteristics are measured in air at room temperature, $W=1$ mm. (b) P3HT, $W=1$ mm, in vacuum at room temperature after a thermal dedoping treatment (see Ref. 6). The insets show the corresponding μ_{FE} values derived from the gatesweeps by using Eq. (1).

The field-effect mobilities for both PTV and P3HT are found to depend on the channel length of the transistor, which can be seen from the insets of Fig. 1. By comparing the output characteristics multiplied by the channel length, that is, at constant source–drain field, for short- and long-channel transistors, we clearly see an effective current decrease for shorter channel lengths, which is demonstrated for P3HT in Fig. 2. Furthermore, at low drain voltages, the output characteristics of the long transistor show ohmic behavior,[8] whereas for the short-channel transistors, at low drain voltages, superlinear output characteristics are observed. Because μ_{FE} is decreasing with reduced L, the reduction of the channel length will not result in the expected increase of the switching speed in circuits.

From amorphous silicon TFTs, it is well known that the presence of source and drain parasitic resistances, R_s and R_d, respectively, can give rise to an apparent μ_{FE} that decreases with decreasing channel length.[9,10] This is due to the fact that in shorter channels, a relatively larger fraction of the applied source–drain voltage drops over the parasitic resistance, as compared with the long-channel transistors. To be able to evaluate the performance of the organic semiconductor, a correction for the parasitic resistance, $R_p=R_s+R_d$, is required.[11,12] A theoretical approach to this end was presented by Horowitz *et al.*[13] Experimentally, it has been demonstrated that the influence of R_p can be reduced by modifying the interface between the current injecting contacts and the organic semiconductor.[14,15] For experimental evaluation of R_p, Kelvin probe force microscopy[8] has been employed. Here, we investigate the scaling behavior of the transistor current[10,16,17] to estimate R_p.

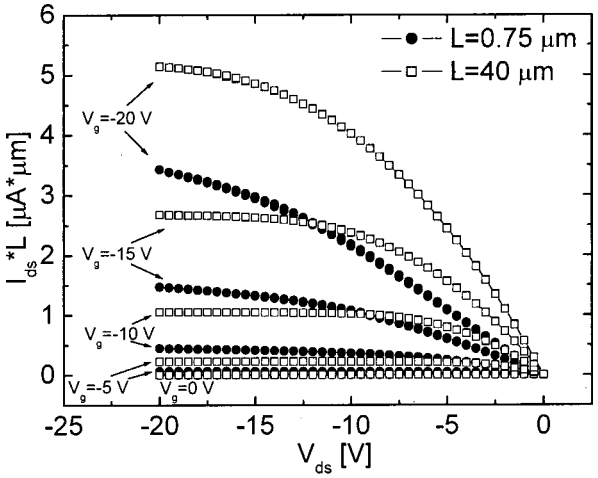

FIG. 2. The normalized output characteristics for two P3HT transistors with $L=0.75$ μm (closed circles) and $L=40$ μm (open squares). Clearly the current in the short transistor is more dominated by the parasitic series resistance as compared to the long transistor.

We plot the total device resistance, $R_{ON}=V_{ds}/I_{ds}$, as a function of the nominal channel length L, for different gate voltages in Fig. 3. In the linear operating regime of the transistor, the channel resistance varies linearly with the channel length. The parasitic resistance, $R_p=R_s+R_d$, at the source and drain contacts is assumed to be independent of L. The R_{ON} can then be expressed as:[10]

$$R_{ON}(L)=\left.\frac{\partial V_{ds}}{\partial I_{ds}}\right|_{V_{ds}\to 0,V_g}=R_{ch}(L)+R_p. \tag{2}$$

The experimental data are, in first order, well described by this equation, with R_{ON} depending linearly on L (see Fig. 3).

From the slopes of the plots in Fig. 3, we find the channel resistance R_{ch}, the inverse of which, $[\Delta R_{ON}/\Delta L]^{-1}$, is the channel conductivity. From the derivative of the channel conductivity, the field-effect mobility, corrected for R_p, can be obtained:

$$\frac{\partial\left[\left(\frac{\Delta R_{ON}}{\Delta L}\right)^{-1}\right]}{\partial V_g}=\mu_{FE}(V_g)WC_i. \tag{3}$$

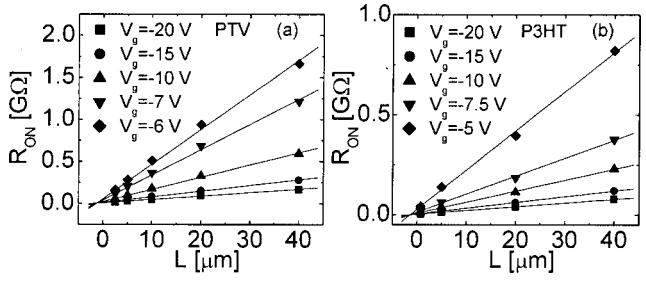

FIG. 3. Total device resistance R_{ON}, calculated with Eq. (2) from the data in Fig. 1, as a function of the channel length for various gate voltages, for (a) PTV and (b) P3HT.

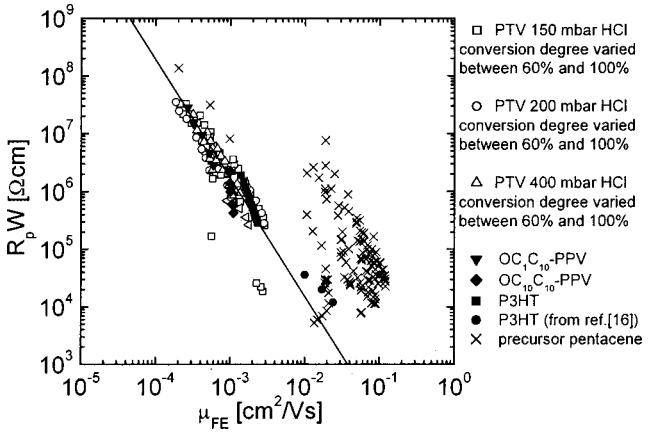

FIG. 4. The parasitic resistance times the channel width as a function of the effective field-effect mobility for a number of polymeric semiconductors and pentacene. The drawn line is a guide for the eye.

The resulting corrected mobilities are plotted in the insets of Fig. 1. The corrected curve yields a higher overall $\mu_{\mathrm{FE}}(V_g)$. From the insets of Fig. 1(b), it is clear that for the 40-μm channel, the influence of R_p is small, as μ_{FE} obtained from Eq. (1) is close to the corrected mobility. We note that any nonlinearity of μ_{FE} with V_g in our samples can not be *a priori* attributed to the presence of an R_p,[13] but is more probably the result of a specific density of states in the semiconductor at the semiconductor/insulator interface. From the analysis with Eq. (2), we find R_p in Fig. 3 as the intercept of R_{ON} at $L=0$. This R_p, typically on the order of $M\Omega$ for our devices, is found to decrease with increasing gate voltage, that is, with increasing carrier density.

We find experimentally that both the field-effect mobility and the parasitic resistance depend on V_g. In Fig. 4, we plot the experimentally determined R_p, multiplied with the channel width, and effective μ_{FE} obtained from the scaling analysis of several organic semiconductors. In addition, data from a P3HT study of Sirringhaus *et al.*[11] are included. An empirical relation is observed between the mobility and the parasitic resistance for the polymeric TFTs in contact with the gold/titanium stack. A possible reason for this empirical observation is that the density of localized states in the polymer is of importance for the charge injection efficiency. Why this results in a very similar dependence of μ_{FE} on R_p for different polymeric semiconductors is unclear at present. In literature it has been demonstrated that injection-limited current into a disordered polymer can be described by thermally assisted hopping from the electrode into the localized states of the polymer, which are broadened due to disorder.[18] As a representation of this effect, the R_p for injection into a semiconducting polymer is found to depend on the charge carrier mobility in the polymer.[19] For the molecular semiconductor pentacene, the data are more scattered, and do not follow the trend observed for the polymeric transistors (see Fig. 4). We attribute this to the polycrystalline nature of the pentacene films, which depends on the processing conditions.

The origin of the observed parasitic series resistance, or injection-limited current, can be due to a combination of effects. In general, geometrical or morphological contact problems between the semiconductor film and the gold contacts can be of importance, which is indicated by the scattered pentacene data. However, the data for the polymers are much more consistent, and suggest that the injection barrier is related to material parameters of electrode and semiconductor layer rather than processing variations. A mismatch between the work function of the gold, at 5.1 eV, and the highest occupied molecular orbital level of the semiconductors (for the materials used here: around 5.2 eV) would lead to an injection barrier for holes. The width of this injection barrier can be narrowed by accumulating charge in the semiconductor, through the field effect, by applying a V_g.[20] For a small barrier height, in the order of the thermal energy $k_{\mathrm{B}}T$, this will result in an ohmic parasitic resistance, whereas for higher barrier heights, a nonohmic parasitic resistance will be present at the electrode/semiconductor interface.

In conclusion, we have used channel-length-dependent measurements to experimentally determine the effective field-effect mobility, corrected for parasitic series resistance, in a variety of spin-coated organic field-effect transistors. For the investigated transistors, we extract a parasitic series resistance, which depends on V_g. This parasitic resistance is attributed to an injection barrier with a height on the order of a few times $k_{\mathrm{B}}T$, which results in an ohmic parasitic series resistance. Experimentally, we find that the parasitic resistance decreases with increasing charge carrier mobility for the investigated polymeric field-effect transistors.

The authors acknowledge M. Matters and E. Cantatore for useful discussions, and the Dutch Science Foundation NWO/FOM for financial support.

[1] G. H. Gelinck, T. C. T. Geuns, and D. M. de Leeuw, Appl. Phys. Lett. **77**, 1487 (2000).
[2] H. E. A. Huitema, G. H. Gelinck, J. B. P. H. van der Putten, K. E. Kuijk, C. M. Hart, E. Cantatore, P. T. Herwig, A. J. J. M. van Breemen, and D. M. de Leeuw, Nature (London) **414**, 599 (2001).
[3] A. R. Brown, C. P. Jarrett, D. M. de Leeuw, and M. Matters, Synth. Met. **88**, 37 (1997).
[4] H. Fuchigami, A. Tsumura, and H. Koezuka, Appl. Phys. Lett. **63**, 1372 (1993).
[5] M. Matters, D. M. de Leeuw, P. T. Herwig, and A. R. Brown, Synth. Met. **102**, 998 (1999).
[6] D. B. A. Rep, B.-H. Huisman, E. J. Meijer, P. Prins, and T. M. Klapwijk, Mater. Res. Soc. Symp. Proc. **660**, JJ7.9 (2001).
[7] E. J. Meijer, C. Tanase, P. W. M. Blom, E. van Veenendaal, B.-H. Huisman, D. M. de Leeuw, and T. M. Klapwijk, Appl. Phys. Lett. **80**, 3838 (2002).
[8] L. Bürgi, H. Sirringhaus, and R. H. Friend, Appl. Phys. Lett. **80**, 2913 (2002).
[9] M. Shur and M. Hack, J. Appl. Phys. **55**, 3831 (1984).
[10] S. Luan and W. Neudeck, J. Appl. Phys. **72**, 766 (1992).
[11] H. Sirringhaus, N. Tessler, D. S. Thomas, P. J. Brown, and R. H. Friend, Festkoerperprobleme **39**, 101 (1999).
[12] L. Torsi, A. Dodabalapur, and H. E. Katz, J. Appl. Phys. **78**, 1088 (1995).
[13] G. Horowitz, R. Hajlaoui, D. Fichou, and A. El Kassmi, J. Appl. Phys. **85**, 3202 (1999).
[14] J. Wang, D. J. Gundlach, C. C. Kuo, and T. N. Jackson, *41st Electronic Materials Conference*, Santa Barbara, California, 30 June–2 July 1999, p. 16.
[15] Y. Y. Lin, D. J. Gundlach, and T. N. Jackson, Mater. Res. Soc. Symp. Proc. **413**, 413 (1996).
[16] K. Terada and H. Muta, Jpn. J. Appl. Phys. **18**, 953 (1979).
[17] J. G. J. Chern, P. Chang, R. F. Motta, and N. Godinho, IEEE Electron Device Lett. **1**, 170 (1980).
[18] T. van Woudenbergh, P. W. M. Blom, M. C. J. M. Vissenberg, and J. N. Huiberts, Appl. Phys. Lett. **79**, 1697 (2001).
[19] Y. Shen, M. W. Klein, D. B. Jacobs, J. C. Scott, and G. G. Malliaras, Phys. Rev. Lett. **86**, 3867 (2001).
[20] S. M. Sze, *Physics of Semiconductor Devices* (Wiley, New York, 1981).